CrossMark

LETTER

Platinum-group elements and minerals in the lower and middle group chromitites of the western Bushveld Complex, South Africa

Malte Junge[1] · **Thomas Oberthür**[1] · **Inga Osbahr**[2] · **Paul Gutter**[3]

Abstract The chromitites of the Bushveld Complex in South Africa contain vast resources of platinum-group elements (PGE). However, knowledge of the distribution and the mineralogical siting of the PGE in the lower group (LG) and middle group (MG) chromitite seams of the Bushveld Complex is limited. We studied concentrates from the LG-6 and MG-2 chromitites of the western Bushveld Complex by a variety of microanalytical techniques. The dominant PGM are sulfides, namely laurite, cooperite-braggite, and malanite-cuprorrhodsite, followed by PGE-sulfarsenides, sperrylite, and Pt-Fe alloys. Laurite is the most abundant PGM (vol%). The matching sets of PGM present in the LG and MG chromitites of both the western and the eastern Bushveld Complex, and in the UG-2 chromitite, show strong similarities which support the assumption of a characteristic and general chromitite-related PGM assemblage. Palladium and Rh contents in pentlandite are low and erratic although maximum contents of 7730 ppm Pd and 6020 ppm Rh were detected.

Editorial handling: M. Fiorentini

✉ Malte Junge
   malte.junge@bgr.de

1 Federal Institute for Geosciences and Natural Resources (BGR), Stilleweg 2, D-30655 Hannover, Germany

2 Helmholtz Institute Freiberg for Resource Technology, Halsbrücker Strasse 34, 09599 Freiberg, Germany

3 SYLVANIA Platinum Ltd., P.O. Box 976, Florida Hills 1716, South Africa

Rare thiospinels of the polydymite-linnaeite-greigite series have PGE contents of 1430 ppm Pt, 5370 ppm Rh, and 1460 ppm Pd. The various PGE occur in different deportment: Platinum is generally present in the form of discrete PGM (sulfides, arsenides, alloys). Palladium is present as a large variety of discrete PGM and also incorporated in pentlandite. Rhodium forms discrete PGM and is occasionally present in pentlandite. The IPGE (Os, Ir, and Ru) are dominantly incorporated in laurite (often as inclusions in chromite) and also occur as sulfarsenides.

Introduction

The 2050 Ma old (Scoates and Friedman 2008) Bushveld Complex in South Africa is the largest layered mafic-ultramafic intrusion on Earth and contains the largest resources of platinum-group elements (PGE) on Earth as well as economically important reserves of chromium and vanadium (Von Gruenewaldt 1977; Vermaak 1995; Zientek et al. 2014). The PGE mineralization in the Bushveld Complex is mainly confined to a layered sequence of mafic-ultramafic rocks referred to as the Rustenburg Layered Suite which is subdivided into the Marginal, Lower, Critical, Main, and Upper Zones (Hall 1932). Today's economic PGE deposits are three major ore bodies, namely the Merensky Reef, the Platreef, and the UG-2 chromitite, the only chromitite layer in the Bushveld Complex mined for PGE as the primary economic metal. However, all chromitite seams contain elevated PGE concentrations ranging from 0.5 to 9 g/t (e.g., Cawthorn 1999; Naldrett et al. 2012). Sylvania Platinum Ltd. is reworking chromite dumps from the LG-6 and MG-1/2 chromitites from the eastern and western Bushveld Complex and successfully produces saleable concentrates of both PGE and chromite. The recovery of PGE as a byproduct from both

active chromite mining operations and reworking of old chromite mine dumps from the lower group (LG) and middle group (MG) chromitites is therefore an excellent opportunity to add value to the primary chromite resources.

The samples of this study were obtained from the recovery plants of Sylvania Platinum Ltd. in the western Bushveld Complex (Fig. 1). The feed material for the PGE concentrates mainly originates from the chrome tailings dumps of the about 1-m-thick LG-6 chromitite at the Millsell and from the about 0.5-m-thick MG-2 chromitite at the Mooinooi operation, as well as from the recent mine production from the nearby Millsell and Mooinooi plants. The PGE-enriched concentrates from the flotation of the chrome dumps material from both plants were studied in detail to unravel the deportment of the PGE and the nature of the platinum-group minerals (PGM) in the ores.

This work is a complementary study to our earlier investigation on the LG/MG chromitites of the eastern Bushveld Complex (Oberthür et al. 2016). The aims of the study are (i) to determine the distribution of the PGE in the LG-6 and MG-2 chromitites, (ii) to determine the PGM assemblages using automated mineralogical analysis, (iii) to acquire data on the concentrations of PGE in sulfides, and (iv) to compare the obtained data with published work on the eastern Bushveld Complex. So far, little information exists on the distribution of PGE and the PGM assemblage of the LG and MG chromitites. Automated mineralogy techniques as used in this study provide statistically robust data on the mode of occurrence of PGM in these chromitite seams which is also of value to the metallurgical treatment of the ores. The new information also conveys valuable knowledge on PGE fractionation processes in general, PGM assemblages in chromite environments, and the partitioning of semimetals between monosulfide solid solution (mss) and sulfide melt.

Previous work

The correlation between chromite and PGE is remarkably well expressed in the Bushveld Complex; even the thinnest chromitite stringers contain elevated concentrations of PGE (e.g., Maier et al. 2013). The UG-2 chromitite has been investigated in great detail (e.g., McLaren and De Villiers 1982; Gain 1985; Hiemstra 1985, 1986; Maier and Barnes 2008; Cawthorn 2011; Junge et al. 2014, 2015a; Osbahr et al. 2014); however, studies on the distribution of PGE and the mineralogical character of the PGM in the LG and MG chromitites are scarce (Lee and Parry 1988; Merkle 1992; Teigler and Eales 1993; Naldrett et al. 2009, 2012; Kotzé and Gauert 2014; Oberthür et al. 2016).

Regarding PGE mineralogy, Lee and Parry (1988) identified laurite as the most common PGM in the MG chromitites, followed by cooperite-braggite, a PdRhCuS phase, PtFe alloys, and PtRhAsS associated with base metal sulfides. Kotzé and Gauert (2014) reported laurite, cooperite-braggite,

and Pt-Fe alloys as the major PGM in a sequence from LG to MG chromitites. A larger number of studies exist for the UG-2 chromitite, which generally agree that the main PGM are cooperite-braggite, laurite, Pt-Fe alloys, and minor malanite/ cuprorhodsite (e.g., Kinloch 1982; McLaren and De Villiers 1982; Viljoen and Schürmann 1998; Schouwstra et al. 2000; Kuhlmann et al. 2006; Junge et al. 2014; Osbahr et al. 2014). Merkle (1992) studied a drill core covering chromitites of the MG of the western Bushveld Complex and showed that the PGM are dominantly sulfides, arsenides, and sulfarsenides and that laurite typically occurs as inclusions in chromite. The PGE mineralogy in sulfide-rich systems such as the Merensky Reef and the Platreef in the Bushveld Complex, as well as the Main Sulfide Zone in the Great Dyke is typically dominated by (Pt,Pd)-bismuthotellurides, cooperite-braggite and minor sperrylite and sulfarsenides (e.g., Oberthür et al. 2003; Holwell and McDonald 2007; Osbahr et al. 2013; Junge et al. 2015b).

Oberthür et al. (2016) studied the distribution of PGM in the LG-6 and MG-1/2 chromitites of the eastern Bushveld Complex and reported that the main PGM are various Pt-Pd-Rh sulfides (cooperite-braggite [(Pt,Pd)S] and malanite/cuprorhodsite [$CuPt_2S_4$]/[$CuRh_2S_4$]), laurite [RuS_2], the main carrier of the IPGE (Os, Ir, Ru), sulfarsenides [(Rh,Pt,Ir)AsS], sperrylite [$PtAs_2$], Pt-Fe-alloys, and a large variety of mainly Pd-rich PGM.

Palladium and Rh contents in sulfides (mainly pentlandite) may range up to thousands of ppm in ores associated with mafic-ultramafic intrusions (Cabri et al. 1984; Cabri 1988; Oberthür et al. 1997, 2003; Osbahr et al. 2013, 2014; Junge et al. 2014, 2015a). In the base metal sulfides of the chromite layer of the Stillwater Complex, Barnes et al. (2016) reported concentrations of Pd, Rh, and Ru in the 250 to 300 ppm range. Oberthür et al. (2016) reported up to some hundred ppm of Pd in pentlandite from the LG and MG chromitites of the eastern Bushveld Complex.

Methodology, samples, and analytical methods

The flotation concentrates were obtained from the recovery plants of Sylvania Platinum Ltd. at Millsell (LG-6 chromitite) and at Mooinooi (MG-2 chromitite) in the western Bushveld Complex (Fig. 1). The feed at Millsell and Mooinooi originates both from current mining operations and from mine dumps. The dump feed at Millsell has an average grade of 1.8 g/t 4E (Pt, Pd, Rh, Au) and the production from the mining operations comprises 8000 t per month. On average, the total feed at Millsell comprises 1.63 g/t 4E at a Cr_2O_3 content of 23 %. Both recovery plants use gravity separation such as spirals and cyclones for the recovery of chromite as well as flotation of the chromite dumps material for the production of PGE concentrates. At Mooinooi and Millsell, a final chromite concentrate with 44 % Cr_2O_3 is produced (Sylvania 2010). More details on the ore processing can be found at the Sylvania website (www.sylvaniaplatinum.com).
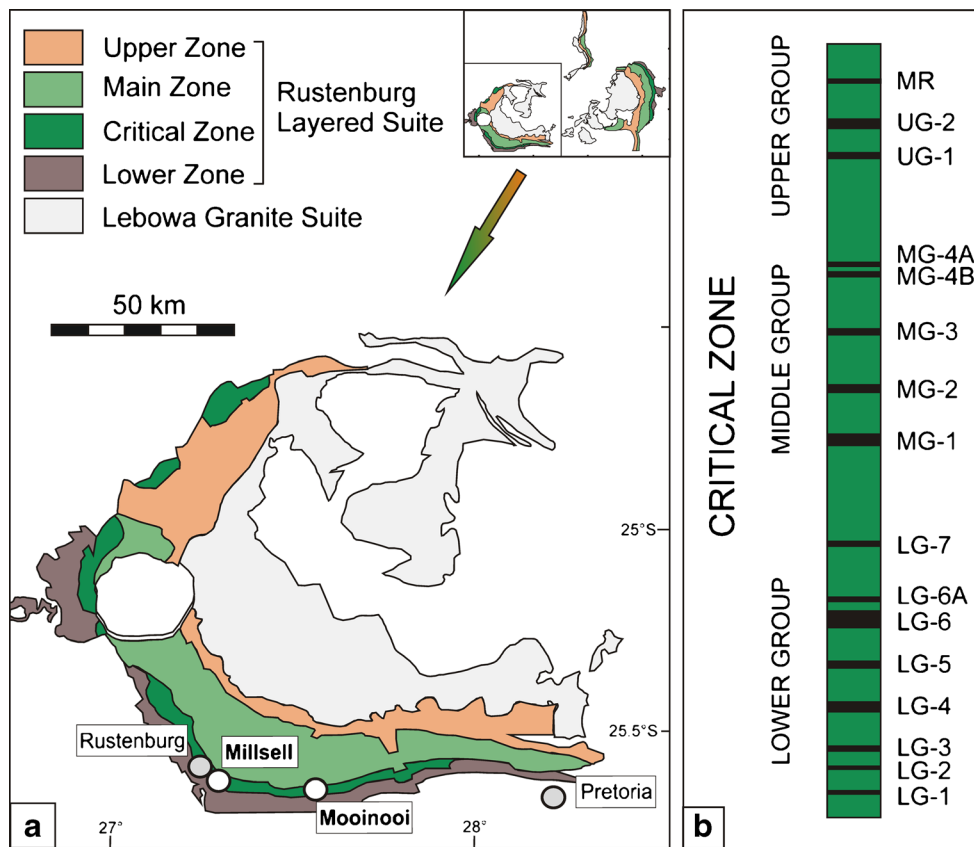
Fig. 1 **a** Geological map of the western Bushveld Complex with the locations of the plants of Sylvania, Millsell and Mooinooi. **b** Schematic stratigraphic column of the critical zone showing the chromitite seams and the Merensky Reef (*MR*). Modified after Oberthür et al. (2016)

The concentrates were analyzed for PGE by ACTLABS, Canada, using nickel sulfide fire assay followed by instrumental neutron activation analysis (INAA). For the INAA method, three different Merensky Reef reference materials from the African Mineral Standards (AMIS0254, AMIS0367, and AMIS0396) were used. Nickel and Cu concentrations are determined by ICP-MS and S contents by ICP after sodium peroxide fusion. For Ni and Cu, a jasperoid (GXR-1) and a porphyry copper ore (GXR-4) from the US Geological Survey and, for S analysis, a zinc-tin-copper-lead ore from Mount Pleasant mine (MP-1b) from the Canadian Certified Reference Materials Project were used as reference material. The results of the reference materials are given in the electronic appendix. Polished sections were prepared for reflected light microscopy, scanning electron microscope (SEM), and microprobe work at BGR in Hannover.

Quantitative mineralogical analysis using the Mineral Liberation Analyzer (MLA) software was carried out using a FEI-Quanta 650 F field emission scanning electron microscope (FE-SEM) equipped with two Bruker Quantax X-Flash 5030 energy dispersive X-ray spectroscopy (EDS) detectors and FEI's MLA suite 3.1.4 software for data acquisition, at the Helmholtz Institute Freiberg for Resource Technology, Germany. In-depth information on the MLA system and PGM identification can be found in Fandrich et al. (2007), Gu (2003)

and Osbahr et al. (2015). In the present study, the sparse phase liberation (SPL)-lite measurement mode was applied for the identification of PGM grains with high spatial resolution and accuracy (Fandrich et al. 2007). In this mode, a series of BSE images is collected and only mineral grains matching defined gray-scale ranges are analyzed by EDS. A summary of tangible instrumental parameters is given in Table 1. Polished sections of the concentrates were analyzed in a first run then re-ground and re-polished and analyzed again in a second run.

Pentlandite grains were analyzed with a CAMECA SX 100 electron microprobe using the following analytical conditions: 20 kV acceleration voltage, 120 nA probe current, and up to 180 s measuring time (backgrounds are half time of peak). The following elements were analyzed: Al (Kα), Si(Kα), S(Kα), Cr(Kα), Fe(Kα), Co(Kα), Ni(Kα), Cu(Kα), As(Lα), Se(Lα), Rh(Lα), Pd(Lα), Ag(Lα), and Pt(Lα). Synthetic metals (for Si, Cr, Pd, Rh, Pt, Ag, Co, Se), natural pentlandite (S, Fe, Ni), chalcopyrite (Cu), synthetic gallium-arsenide (As), and chromite (Al) were used as standards. Average detection limits were 75 ppm for Co, 100 ppm for Se, 120 ppm for Rh, 140 ppm for Pd, 160 ppm for Ag, and 300 ppm for Pt. Corrections were performed using the PAP program supplied by CAMECA, and further interferences were corrected using a spreadsheet developed at BGR.

Table 1 Summary of MLA parameters

SEM parameters		MLA parameters	
Voltage [kV]	25	Scan speed	16
Working distance [mm]	13	Resolution [px]	1000×1000
Probe current [nA]	10	Pixel size (µm/px)	0.6
Spot size[a]	5.704	Acquisition time [ms]	5
Horizontal field width [µm]	600	SPL BSE trigger	95–255
Brightness	93.77	Minimum grain size [px]	2
Contrast	19.40		
BSE calibration	Au 245		

[a] Spot size of 5.704 equates to a ca. 10-nm beam diameter

Results

Geochemistry

Bulk analyses (PGE, Au, Ni, Cu, and S) of the PGE flotation concentrates from Millsell (LG-6) and Mooinooi (MG-2) are presented in Table 2. The Pt/Pd, Pd/Ir, and PPGE/IPGE (Rh, Pt, Pd/Os, Ir, Ru) ratios are similar at Millsell and Mooinooi and are all above unity. C-1 chondrite-normalized PGE distribution patterns of both the Millsell and the Mooinooi concentrates (Fig. 2) display positive slopes from Os to Rh and a drop from Pt to Pd. These patterns are largely parallel to those of the chrome tailings dumps, the feed material for the PGE concentrates, from Millsell and Mooinooi, as well as to those of the LG-6, MG-1, MG-2, and UG-2 chromitites presented in the literature (Scoon and Teigler 1994; Junge et al. 2014) and the data of four concentrates of the LG-6 and MG-1/2 from the eastern Bushveld (Oberthür et al. 2016), indicating that no apparent fractionation takes place during ore processing. The similar distribution pattern between the Millsell and Mooinooi concentrates with the respective tailing and literature data allows the comparison of the PGE and PGM distribution between the LG-6 and MG-1/2 chromitites.

Mineralogy

According to X-ray diffraction analysis, the main mineral components of both flotation concentrates (Millsell and Mooinooi) are talc and minor chlorite/vermiculite, calcite, and orthopyroxene. Ore microscope and SEM studies showed that the sulfides (chalcopyrite, pentlandite, pyrite, and rare millerite) and the PGM are largely liberated in the concentrates and occur as single grains or in grain aggregates (Fig. 3). Sulfide grain aggregates range in size from <1 to about 60 µm.

Mineral liberation analysis

Our mineral liberation analysis (MLA) application subdivides major groups of PGM into PGE-sulfides (malanite, cooperite, braggite, laurite, and vysotskite), PGE-sulfarsenides (irarsite and hollingworthite), Pt-Fe-alloys (iso- and tetraferroplatinum), zvyagintsevite, and sperrylite. Cooperite, braggite, and vysotskite are grouped as *PGE-sulfides* [(Pt,Pd)S] in the following and the members of the malanite-cuprorhodsite solid solution series as *malanite* (Fig. 4).

The number of grains, the areas occupied in square micrometers, and grain sizes are important factors in describing the PGM and their distribution in the ores. In the LG-6, grain sizes of the PGM range from 2 to 20 µm, and laurite may reach up to 35 µm. In the MG-2, the PGM show similar grain sizes (up to 15 µm); however, Pt-Fe alloys represent the biggest grains with up to 45 µm in diameter.

Mineral proportions of the PGM (number of grains and areas, in %) in the Millsell (LG-6) and Mooinooi (MG-2) concentrates are shown in Fig. 5. By number of grains, malanite is the most dominant phase (25 to 29 %) both at Millsell and Mooinooi, followed by PGE-sulfarsenides (18 to 20 %). Common are laurite (14 to 16 %) and [(Pt,Pd)S] (Millsell 13 %, Mooinooi 11 %, respectively), and sperrylite makes up 9 and 10 % at Millsell and Mooinooi, respectively, whereas Pt-Fe alloys comprise 3 and 4 %, respectively. Zvyagintsevite [Pd_3Pb] and stibiopalladinite [$Pd_{5 + x}Sb_{2 - x}$] are minor constituents (<2 %). Other PGM like moncheite [$PtTe_2$], potarite [PdHg], and atokite [Pd_3Sn] together represent around 10 %.

Considering area %, laurite is the most dominant phase at both locations (24 % at Millsell and 28 % at Mooinooi), followed by malanite (22 and 20 %), [(Pt,Pd)S] (12 and 16 %), PGE-sulfarsenides (12 %), and sperrylite (11 and 8 %).

It has to be kept in mind that the concentrates have experienced various stages of crushing, milling, sieving, and finally flotation. Also due to this fact, a large number of grains show free surfaces, namely 52 % in the MG-2 and even 67 % in the LG-6. Laurite is often observed as inclusions in chromite (e.g., Merkle 1992; Penberthy et al. 2000; Junge et al. 2014; Oberthür et al. 2016). A certain proportion of these laurite grains is liberated during ore processing of the chromitite and show free surfaces in the concentrate. The amount of PGM associated with chromite in the original ore is therefore

Table 2 Bulk analysis data of PGE, Au, Ni, Cu, and S, as well as Pt/Pd and PPFE/IPGE ratios of flotation concentrates of Millsell and Mooinooi from the plants of Sylvania Platinum Ltd. (analyzed by ACTLABS, Canada)

	Os [ppb]	Ir [ppb]	Ru [ppb]	Rh [ppb]	Pt [ppb]	Pd [ppb]	Au [ppb]	Ni [ppm]	Cu [ppm]	S [wt.%]	Pt/Pd	Pd/Ir	PPGE/IPGE	∑PGE [ppm]
Millsell (LG-6)	2170	4520	19,700	7890	57,200	20,000	145	1790	1010	0.33	2.86	4.42	3.22	111.5
Mooinooi (MG-2)	1950	4010	17,100	7320	48,200	17,500	145	1690	863	0.37	2.75	4.36	3.16	96.1

probably larger than shown in the concentrates. As at least part of the free surfaces represents cracks from crushing, only the remaining PGM grains were taken into consideration in discussing mineral associations. These PGM are mostly associated with silicates (54 and 60 % in the LG-6 and MG-2, respectively), followed by sulfides (37 and 32 % in the LG-6 and MG-2, respectively). Rarer associations are with chromite (2 %) or other PGM (5 to 7 %). Less than 1 % of the PGM are associated with carbonates, Fe oxides, or rutile (Fig. 6).

PGE in sulfides

The presence of elevated concentrations of Pd and Rh in sulfides (mainly pentlandite) ranging from some 100 ppm to a few wt% was shown in PGE ores from the Bushveld Complex (e.g., Godel et al. 2007; Holwell and McDonald 2007, 2010;

Osbahr et al. 2013, 2014; Junge et al. 2014, 2015a). In the present study of pentlandite grains from Millsell (LG-6) and Mooinooi (MG-2) (both $n = 13$), average contents of 385 and 1005 ppm Pd, respectively, were determined. Maximum contents in pentlandite were 7730 ppm Pd and 6020 ppm Rh. Furthermore, for the first time, PGE contents were analyzed in some rare thiospinel grains of the polydymite-linnaeite-greigite series. In a grain with composition close to siegenite [$Ni_{1.5}Co_{1.2}Fe_{0.4}S_4$], 1430 ppm Pt were detected, and a grain with the composition [$Ni_{2.2}Fe_{0.5}Cu_{0.3}S_4$] had 5370 ppm Rh and 1460 ppm Pd.

Summary and discussion

The chondrite-normalized PGE distribution pattern of the flotation concentrates from the LG-6 and MG-2
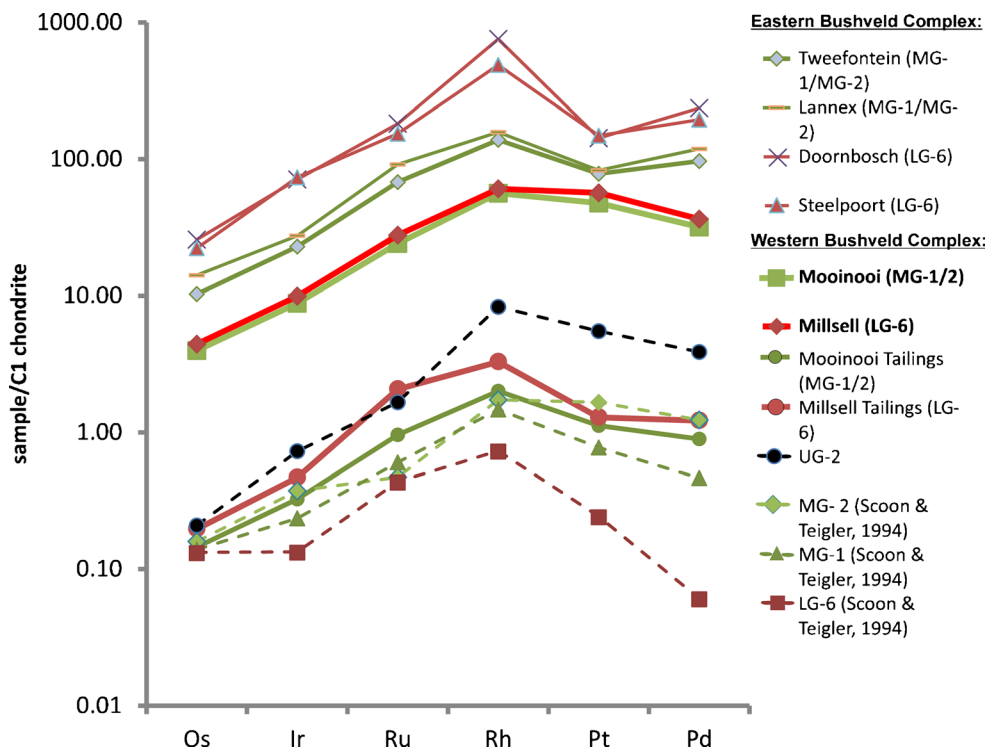

Fig. 2 Chondrite normalized PGE-distribution pattern of Millsell (LG-6) and Mooinooi (MG-2) of the western Bushveld Complex. For comparison, flotation concentrate PGE data from processing plants of the LG-6 and MG-1/2 of the eastern Bushveld Complex (Oberthür et al. 2016) and whole-rock data from the LG-6, MG-1, MG-2 (all Lee and Parry 1988) and UG-2 (Junge et al. 2014) from the literature is plotted. C1-chondrite values are taken from McDonough and Sun (1995)
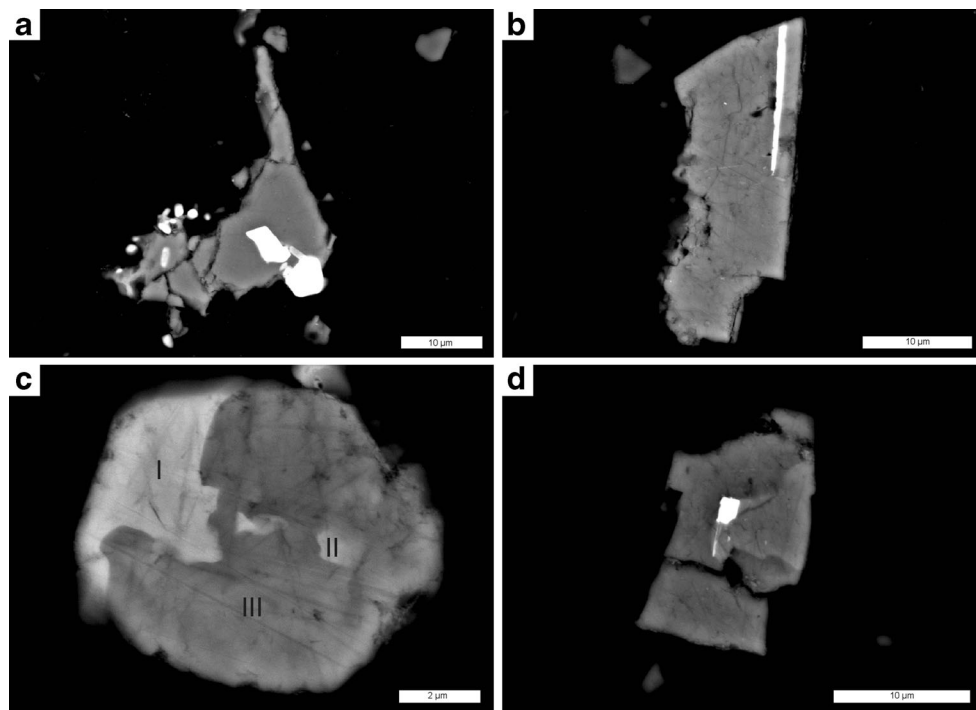
Fig. 3 Back-scattered electron images of sulfide and PGM grains. **a** Grains of hollingworthite (*white*) in pyrite (*gray*). **b** Malanite (*white*) in pentlandite (*gray*). **c** Sperrylite (*I*), stibiopalladinite (*II*), and hollingworthite (*III*). **d** Malanite (*white*) in pentlandite (*medium gray*) and pyrite (*dark gray*)

chromitite, respectively chrome tailings material, from Millsell and Mooinooi and literature bulk-rock data of the LG-6 and MG-2 demonstrate that no preferential upgrade of any PGE has taken place during the flotation process, corroborating findings of Oberthür et al. (2016) on concentrates of the eastern Bushveld Complex. This observation allows the comparison of PGE and PGM distribution of the LG-6 and MG-2 flotation concentrate with the chromitite seams on a statistical basis. LG-6 data of the literature show a negative slope from Rh to Pd which is less pronounced in tailings and concentrates of this study. This may indicate that Pt and Pd are
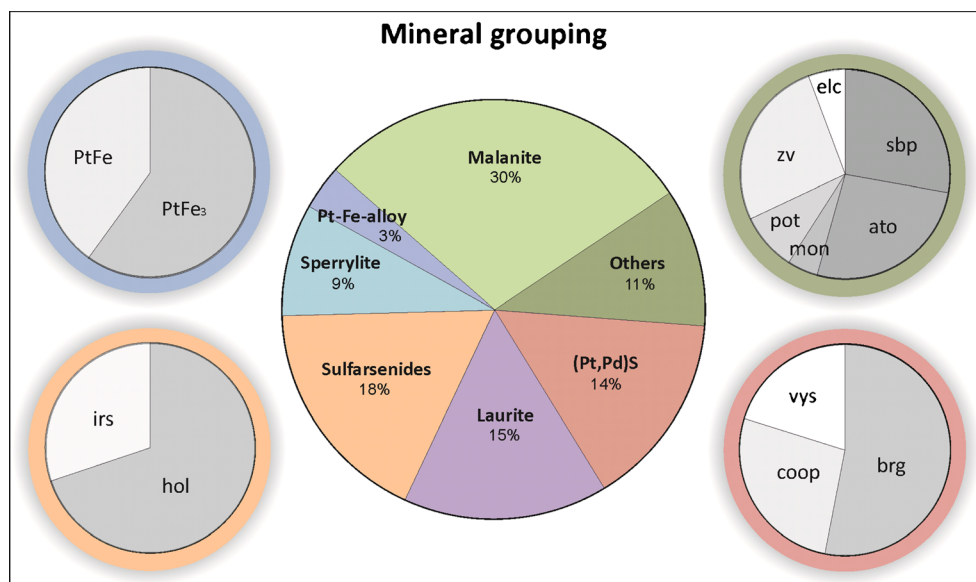

Fig. 4 Structure of mineral grouping of PGM. Example based on grain count data from the LG-6 (Millsell). *Abbreviations*: irarsite (*irs*), hollingworthite (*hol*), zvyagintsevite (*zv*), potarite (*pot*), moncheite (*mon*), atokite (*ato*), stibiopalladintite (*sbd*), electrum (*elc*), vysotskite (*vys*), cooperite (*coop*), braggite (*brg*)
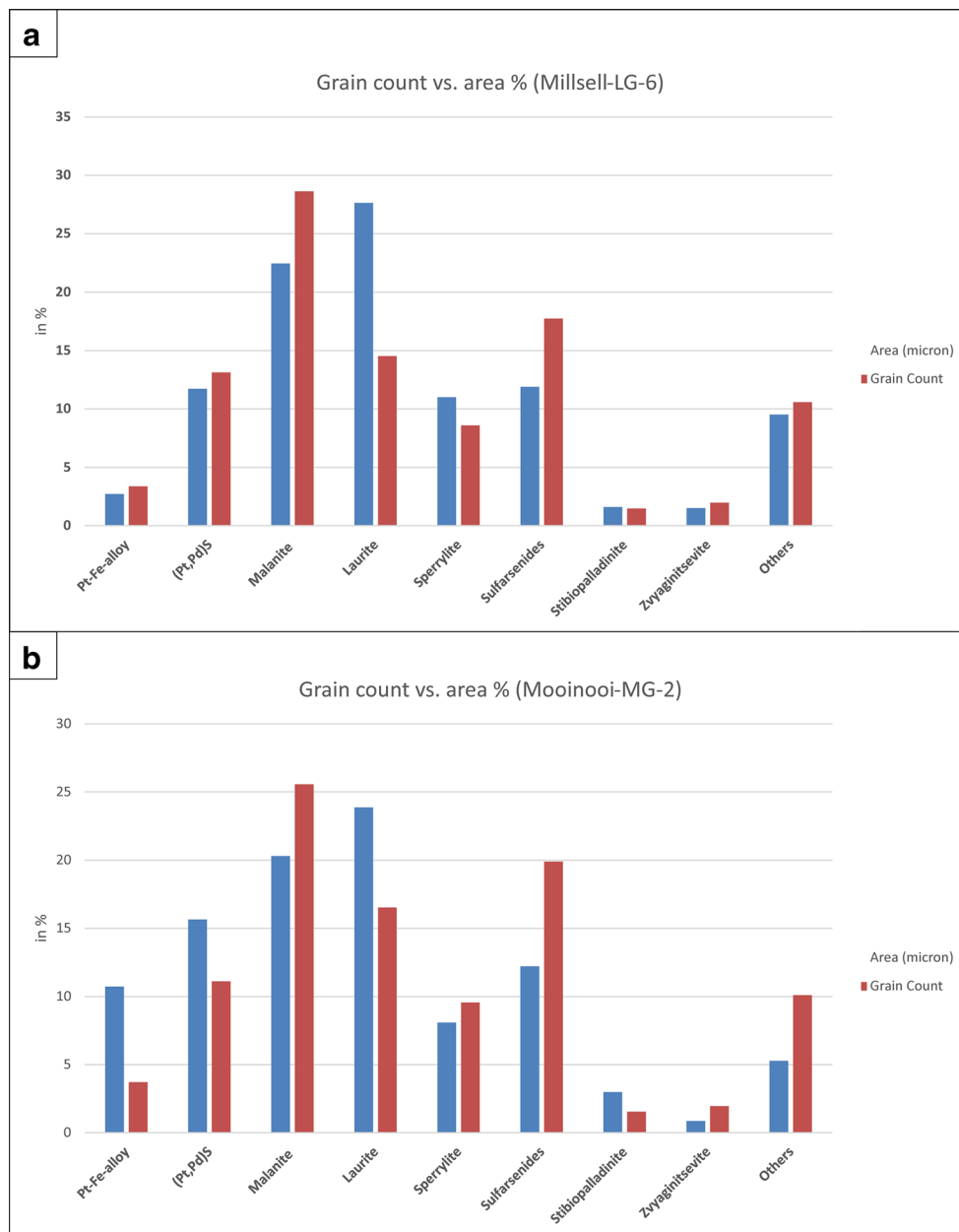
Fig. 5 Number of grains in % from A. Millsell and B. Mooinooi. Area in μm^2 normalized to 100 % PGM

relatively stronger enriched in the tailings and concentrates than Os, Ir, Ru, and Rh.

Ore microscopy and SEM/MLA studies usually report the number of PGM grains only. However, modern analytical methods also allow determining area percentages of the various PGM. This important advance assists in the interpretation of data as one single large PGM grain can account for tens or hundreds of smaller PGM, and therefore, large PGM would be under-emphasized compared to more abundant but substantially smaller PGM although these have a minor impact on the bulk PGM content and the bulk metal budget (Cabri 2015). In our samples, the comparison of grain frequency and area percentage shows that, e.g., laurite grains are on average larger

than sulfarsenides, but there are relatively more grains of sulfarsenides. Laurite grains often occur as inclusions in chromite (e.g., Junge et al. 2014) and, as this PGM assemblage is based on flotation concentrates, small-sized laurite grains may not all be separated during processing.

Newly calculated area percentages of the PGM assemblages of LG and MG chromitites of the eastern Bushveld Complex presented by Oberthür et al. (2016) are shown in the electronic supplementary appendix. Similar to Millsell and Mooinooi, the LG and MG chromitites of the eastern Bushveld Complex (LG-6: Doornbosch, Steelpoort and MG-1/2: Lannex, Tweefontein), laurite is overemphasized and sulfarsenides are underrated with respect to the area percentage. Further, malanite has a larger
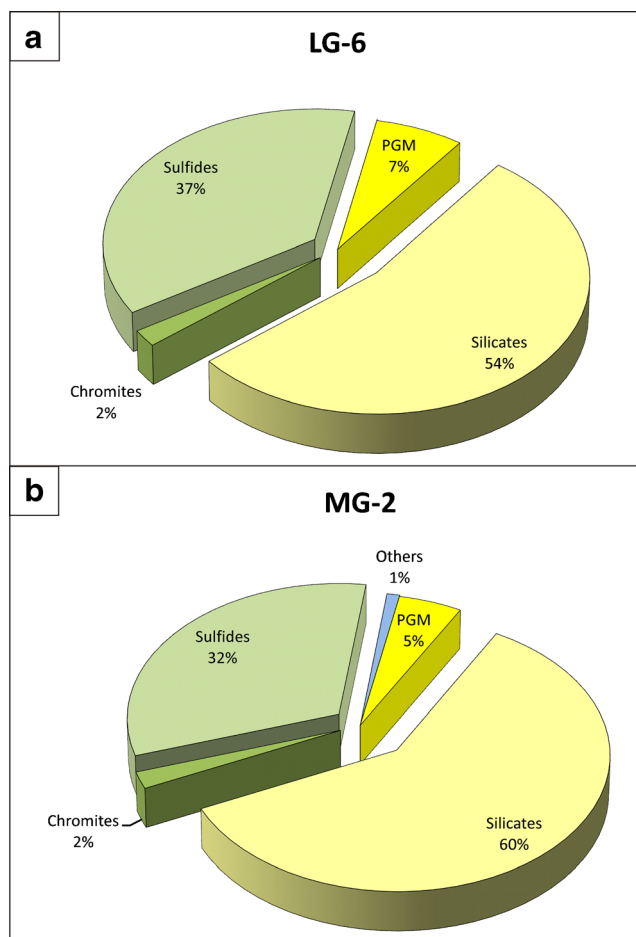
Fig. 6 Mineral association proportions based on MLA data. **a** PGM concentrate from Millsell (LG-6). **b** PGM concentrate from Mooinooi (MG-2). Mineral associations without free surface are normalized to 100 %

area percentage than frequency percentage data in the LG-6 than in the MG-1/2 chromitites, arguing that malanite has an even larger influence on the bulk potential of PGM and the metal budget in the system in the LG-6 chromitites of the eastern Bushveld Complex than shown by frequency data only.

The PGM assemblages of the LG-6 and MG-2 chromitite samples from the western Bushveld Complex are very similar. However, in comparison with the data from the LG-6 and MG-1/2 chromitites of the eastern Bushveld (Oberthür et al. 2016), the LG-6 and MG-2 chromitites of the western Bushveld generally contain more PGE-sulfarsenides compared to the seams (in particular the LG-6) of the eastern limb. With regard to arsenides and sulfarsenides, the PGM assemblages of Millsell and Mooinooi closely resemble those from Lannex and Tweefontein (both originating from the MG-1/2 chromitites) in the eastern Bushveld Complex.

A comparative summary of the PGM assemblages in LG/ MG chromitites of the eastern and western Bushveld Complex is presented in Fig. 7. Obviously, the differences in PGE

mineralogy between LG and MG chromitites are less pronounced in the western than in the eastern Bushveld. The proportions of PGE-arsenides/sulfarsenides by number of grains in both the LG-6 and MG-1/2 are larger in the western (27 to 30 %) than in the eastern Bushveld (11 to 26 %), although low PGE-arsenides/sulfarsenides occur in the LG-6 of the eastern Bushveld. PGE-sulfides are less abundant in the LG-6 of the western (56 %) than of the eastern Bushveld (68 to 69 %). Also, the amount of Pt-Fe alloys is less pronounced in the eastern (3 to 4 %) compared to the western Bushveld Complex (7 to 12 %). The area percentages show similar results and are given in the ESM.

Despite slight differences, the PGM assemblages of the LG and MG samples from the western Bushveld are akin to those from the eastern Bushveld (Oberthür et al. 2016) and also show far-reaching similarities to samples from the UG-2 chromitite (e.g., Kinloch 1982; Penberthy et al. 2000; Voordouw et al. 2010; Junge et al. 2014; Osbahr et al. 2014). The PGM assemblages are dominated by PGE-sulfides (malanite, laurite, cooperite-braggite), followed by PGE-arsenides, PGE-sulfarsenides, and Pt-Fe alloys. Voordouw et al. (2010) conducted a detailed study of the lateral variation of the PGM assemblage in the UG-2 chromitite and showed that the PGM are mostly cooperite-braggite, Pt-Rh-Cu sulfides (i.e., malanite-cuprorhodsite), laurite, and Pt-Fe alloys. Notably, PGE-bismuthotellurides are nearly absent in the LG and MG chromitites and also in the UG-2 chromitite (this study and Junge et al. 2014; Osbahr et al. 2014). Penberthy et al. (2000) reported that the PGM in the UG-2 are either predominantly associated with base metal sulfides or are locked in chromite or silicate or at grain boundaries between chromite and silicate.

In general, PGE mineralization is associated either with chromitites, or with sulfide-rich rocks, termed as "chromite control" and "sulfide control" (e.g., Scoon and Teigler 1994; Naldrett 2004). Chromitites are typically enriched in IPGE over PPGE (Lee and Parry 1988; Lee 1996; Naldrett 2004). The mode of the occurrence of PGE in a chromite environment is still under debate, i.e., PGE occurring in solid solution in the chromite lattice, or in associated sulfides, or as discrete PGM (inclusions or free grains), or as metal clusters (Tredoux et al. 1995; Naldrett et al. 2009, 2012; Locmelis et al. 2011; Pagé et al. 2012). It is well known that the PGE strongly partition into sulfide compared to silicate liquid due to the high partition coefficients of the PGE, which are on the order of 10^3 to 10^6 (e.g., Campbell et al. 1983; Mungall and Brenan 2014) or even 10^7 to 10^{11} for Pt between sulfide and silicate melt depending on fS_2 and fO_2 (Fonseca et al. 2009). In the Bushveld Complex, the IPGE contents are relatively constant in the chromitites of the Critical Zone, whereas the PPGE steadily increase from the LG-5 upwards (Naldrett and Von Gruenewald 1989; Scoon and Teigler 1994). The abrupt change in PPGE concentrations points to the fact that sulfide
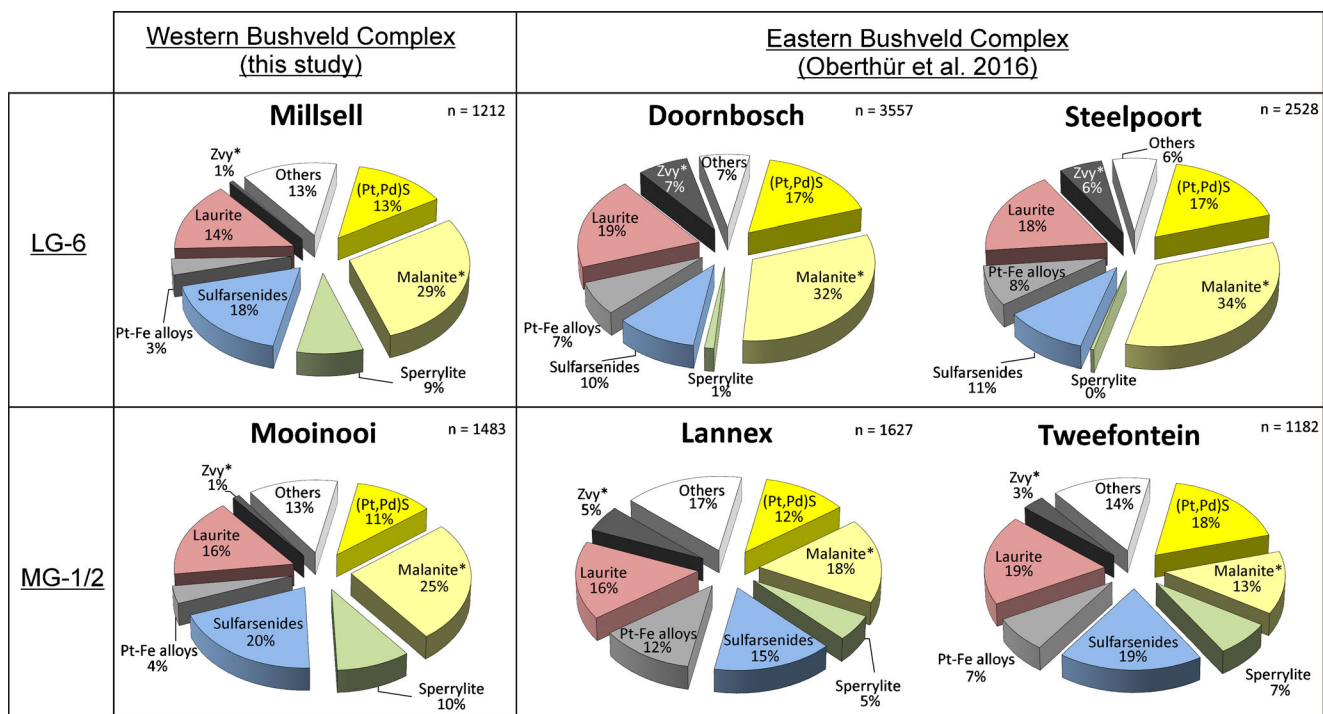
Fig. 7 Frequency percentage of PGM in the chromitite seams of Millsell and Mooinooi (this study) and for comparison of Doornbosch, Steelpoort, Lannex, and Tweefontein (Oberthür et al. 2016; "*n*" equals number of grains)

control took over from chromite control from the LG-5 upwards (Oberthür et al. 2016). The most abundant PGM within the LG-6 and MG-2 in the western Bushveld Complex is laurite (typically Os- and Ir-bearing). The appearance of laurite in chromite as well as experimental studies indicates that laurite may have been formed at magmatic conditions (Brenan and Andrews 2001; Bockrath et al. 2004).

Dominant PGM in Millsell and Mooinooi are sulfides (laurite, malanite-cuprorhodsite, cooperite-braggite) and arsenides (sperrylite and sulfarsenides) totaling 83 % and 82 %, respectively, whereas PGE-bismuthotellurides are missing. PGE mineralization in a chromite environment is generally dominated by PGE-sulfides, PGE-arsenides, and PGE-sulfarsenides. However, within sulfide-rich systems, PGE-bismuthotellurides are the dominant PGM besides cooperite-braggite and sperrylite. Elevated concentrations of As in the initial melt cause As to preferentially associate with PGE, forming PGE-As molecules or polyatomic clusters which are then stabilized during further cooling (Tredoux et al. 1995; Helmy et al. 2010). Besides the metal/sulfur ratio, the partition coefficients $D_{mss/melt}$ of As also strongly depends on fS_2. In relatively reduced sulfide melts, As may be incorporated in the mss or stabilize discrete arsenide minerals (Helmy et al. 2010). The mode of PGE occurrence in chromitites is therefore related to an initially more As-rich environment, allowing the formation of stable high-temperature arsenides and sulfarsenides. In base metal sulfide systems such as the Merensky Reef, the Great Dyke, and the Platreef, PGM are typically (Pt,Pd)-

bismuthotellurides (e.g., Oberthür et al. 2003; Holwell and McDonald 2007; Osbahr et al. 2013; Junge et al. 2015b). The elements Te and Bi are highly incompatible with mss and therefore strongly partition into the sulfide melt (Helmy et al. 2010). PGE-bismuthotellurides must therefore not have formed by solid state exsolution from crystallizing mss but rather may originate from droplets of immiscible Te-Bi-enriched melts (Helmy et al. 2007, 2010). The partition coefficient $D_{mss/melt}$ of As, Te, and Bi also largely depends on the atomic radii as Te and Bi have larger atomic radii than As and S. Within chromite environments, only the semi-metals with smaller atomic radii occur, whereas in sulfide-rich systems, the semi-metals with larger atomic radii and a higher incompatibility in mss form the dominant PGM species. The different PGM assemblages of a chromitite (PGE-sulfides, arsenides, and sulfarsenides) versus a sulfide (PGE-bismuthotellurides, alloys) environment reflect the availability of the semimetals As, Te, and Bi in the melt, the fS_2, and the partition coefficient $D_{mss/melt}$ of As, Te, and Bi.

Pentlandite grains from Millsell (LG-6) and Mooinooi (MG-2) have average contents of 385 and 1005 ppm Pd, respectively, and maximum contents in pentlandite were 7730 ppm Pd and 6020 ppm Rh. PGE contents in thiospinel grains of the polydymite-linnaeite-greigite series were 1430 ppm Pt in a grain with a near-siegenite composition [$Ni_{1.5}Co_{1.2}Fe_{0.4}S_4$] and 5370 Rh and 1460 Pd in a grain with the composition [$Ni_{2.2}Fe_{0.5}Cu_{0.3}S_4$]. These concentrations are based on EPMA data and may reflect either solid solution in

the sulfides or submicrometer-sized inclusions of PGM (see Junge et al. 2015a).

In general, laurite is the dominant carrier of the IPGE and formed at magmatic conditions (Brenan and Andrews 2001; Bockrath et al. 2004). Hollingworthite, the main sulfarsenides and malanite-cuprorrhodite are the major hosts of Rh. Palladium and Rh additionally occur within pentlandite.

Conclusions

(1) The chondrite-normalized PGE patterns of the LG-6 and MG-2 flotation concentrates from Millsell and Mooinooi are similar to the tailings of Millsell and Mooinooi, as well as to literature whole-rock data indicating no strong preferential upgrade of any PGE during the metallurgical processing of the ores and enabling the direct comparison of flotation concentrates with the respective chromitite seams.

(2) Sulfides (chalcopyrite, pentlandite, rare millerite) are scarce and pyrrhotite is largely missing.

(3) In both the Millsell (LG-6) and the Mooinooi (MG-2) PGM-concentrate samples, PGE-sulfides (cooperite-braggite, malanite, laurite) predominate, followed by PGE-sulfarsenides, sperrylite, and Pt-Fe alloys. The LG-6 concentrate has slightly larger contents of PGE-sulfides. PGE-bismuthotellurides are typically missing. In general, laurite is the predominant PGM (area percentage) and the total number can increase as probably not all laurite grains occurring as small inclusions in chromite grains are recovered during flotation.

(4) The PGM assemblages of the LG and MG chromitites of the western and the eastern Bushveld Complex are very similar arguing for the same formation processes.

(5) The similar PGM assemblages of the LG and MG chromitites of the western and the eastern Bushveld Complex and the UG-2 chromitite appear to be "typical" of chromite-rich environments. The different PGM assemblages in a chromitite (PGE-sulfides, arsenides, and sulfarsenides) and sulfide (PGE-bismuthotellurides, PGE-sulfides, alloys) environment reflect differences in fS_2 and in the availability of the semimetals As, Te, and Bi in the melt as well as differences in the partition coefficients $D_{mss/melt}$ of As, Te, and Bi.

(6) Platinum characteristically forms discrete PGM (cooperite-braggite and sperrylite). Palladium occurs in a variety of discrete PGM and incorporated in sulfide (pentlandite). Rhodium is mainly found in the form of discrete PGM (hollingworthite, cuprorrhodite) and is also hosted in pentlandite. The IPGE (Os, Ir, and Ru) are mainly hosted in laurite (often as inclusions in chromite) and are also found in sulfarsenides.

(7) Pentlandite grains from Millsell and Mooinooi have average contents of 385 and 1005 ppm Pd, respectively, and maximum contents of 7730 ppm Pd and 6020 ppm Rh.

(8) PGE contents in thiospinel grains of the polydymite-linnaeite-greigite series showed 1430 ppm Pt in a grain with a near-siegenite composition and 5370 Rh and 1460 Pd in a second grain. These concentrations are analyzed by EPMA and can be the result of both solid solution and submicrometer-sized inclusions of discrete PGM.

References

Barnes S-J, Pagé P, Prichard HM, Zientek ML, Fisher PC (2016) Chalcophile and platinum-group element distribution in the Ultramafic series of the Stillwater Complex, MT, USA—implications for processes enriching chromite layers in Os, Ir, Ru, and Rh. Mineral Deposita 51:25–47

Bockrath C, Ballhaus C, Holzheid A (2004) Stabilities of laurite RuS₂ and monosulfide liquid solution at magmatic temperature. Chem Geol 208:265–271

Brenan JM, Andrews D (2001) High-temperature stability of laurite and Ru-Os-Ir alloy and their role in PGE fractionation in mafic magmas. Can Mineral 39:341–360

Cabri LJ (1988) Applications of proton and nuclear microprobes in ore deposit mineralogy and metallurgy. Nucl Instr & Methods in Physics Research 30:459–465

Cabri LJ (2015) Importance of sample preparation, representivity, and reporting methologies for quantitative evaluation of precious metal mineralogy. Abstract at the Joint Assembly meeting of the AGU-GAC-MAG-CGU, 3–7 May 2015 in Montreal Canada

Cabri LJ, Blank H, El Goresy A, Laflamme JHG, Nobiling R, Sizgoric MB, Traxel K (1984) Quantitative trace-element analyses of sulfides from Sudbury and Stillwater by proton microprobe. Can Mineral 22:521–542

Campbell IH, Naldrett AJ, Barnes SJ (1983) A model for the origin of the platinum-rich sulfide horizons in the Bushveld and Stillwater Complexes. J Petrol 24:133–165

Cawthorn RG (1999) Platinum-group element mineralization in the Bushveld Complex—a critical reassessment of geochemical models. S Afr J Geology 102:268–281

Cawthorn RG (2011) Geological investigations of the PGE distribution in the Bushveld Merensky and UG2 chromite reefs. Journal S Afr Inst Mining Metallurgy 111:67–79

Fandrich R, Gu Y, Burrows D, Moeller K (2007) Modern SEM-based mineral liberation analysis. Int J Miner Process 84:310–320

Fonseca ROC, Campbell IH, O'Neill HSC, Allen CM (2009) Solubility of Pt in sulphide mattes: implications for the genesis of PGE-rich

horizons in layered intrusions. Geochim Cosmochim Acta 73:5764–5777

Gain SB (1985) The geologic setting of the platiniferous UG-2 chromitite layer on the farm Maandagshoek, eastern Bushveld Complex. Econ Geol 80:925–943

Godel B, Barnes S-J, Maier WD (2007) Platinum-group elements in sulphide minerals, platinum-group minerals, and whole-rocks of the Merensky Reef (Bushveld Complex, South Africa): implications for the formation of the reef. J Petrol 48:1569–1604

Gu Y (2003) Automated scanning electron microscope based mineral liberation analysis. J Minerals Materials Characterization and Engineering 2:33–41

Hall AL (1932) The Bushveld igneous complex of the central Transvaal. The Government Printer, Pretoria, 560 pp

Helmy HM, Ballhaus C, Berndt J, Bockrath C, Wohlgemuth-Ueberwasser C (2007) Formation of Pt, Pd and Ni tellurides: experiments in sulfide–telluride systems. Contrib Mineral Petrol 153:577–591

Helmy HM, Ballhaus C, Wohlgemuth-Ueberwasser C, Fonseca ROC, Laurenz V (2010) Partitioning of Se, As, Sb, Te and Bi between monosulfide solid solution and sulfide melt—application to magmatic sulfide deposits. Geochim Cosmochim Acta 74:6174–6179

Hiemstra SA (1985) The distribution of some platinum-group elements in the UG-2 chromitite layer of the Bushveld Complex. Econ Geol 80:944–957

Hiemstra SA (1986) The distribution of chalcophile and platinum-group elements in the UG-2 chromitite layer of the Bushveld complex. Econ Geol 81:1080–1086

Holwell DA, McDonald I (2007) Distribution of platinum-group elements in the Platreef at Overysel, northern Bushveld Complex: a combined PGM and LA-ICP-MS study. Contrib Mineral Petrol 154:171–190

Holwell DA, McDonald I (2010) A review of the behavior of platinum group elements within natural magmatic sulfide ore systems. Platin Met Rev 54:26–36

Junge M, Oberthür T, Melcher F (2014) Cryptic variation of chromite chemistry, platinum group-element and -mineral distribution in the UG-2 chromitite—an example from the Karee Mine, western Bushveld Complex, South Africa. Econ Geol 109:795–810

Junge M, Wirth R, Oberthür T, Melcher F, Schreiber A (2015a) Mineralogical siting of platinum group elements in pentlandite from the Bushveld Complex, South Africa. Mineral Deposita 50:41–54

Junge M, Oberthür T, Kraemer D, Melcher F, (2015b) Distribution of platinum-group elements in pristine and near-surface ores from the Platreef, northern Bushveld Complex, South Africa: Extended abstract 13th Biennial SGA Meeting Nancy, France, p. 955–959

Kinloch ED (1982) Regional trends in the platinum-group mineralogy of the critical zone of the Bushveld Complex, South Africa. Econ Geol 77:1328–1347

Kotzé E, Gauert C (2014) PGE-bearing minerals in chromitites of the Critical Zone (LG-6 to UG-3A) on Winterfeld 293KT, Eastern Bushveld Complex. IMA 2014, Johannesburg, Abstract Volume: 105

Kuhlmann G, Oberthür T, Melcher F, Lodziak J (2006) UG-2 Chromitithorizont – Mineralogisch-Geochemische Feinstratigraphie, Schwerpunkt Platinmetall-Verteilung. Bundesanstalt für Geowissenschaften und Rohstoffe (BGR), Internal Report Tgb.-Nr. 11327/06: 167pp

Lee CA (1996) A Review of Mineralization in the Bushveld Complex and some other Layered Intrusions. In: Cawthorn RG (ed) Layered Intrusions, Elsevier: 103–145

Lee CA, Parry SJ (1988) Platinum-group element geochemistry of the lower and middle group chromitites of the eastern Bushveld Complex. Econ Geol 83:1127–1139

Locmelis M, Pearson NJ, Barnes SJ, Fiorentini ML (2011) Ruthenium in komatiitic chromite. Geochim Cosmochim Acta 75:3645–3661

Maier WD, Barnes S-J (2008) Platinum-group elements in the UG1 and UG2 chromitites, and the Bastard reef, at Impala platinum mine, western Bushveld Complex. South Africa: Evidence for late magmatic cumulate instability and reef constitution: South African Journal of Geology 111:159–176

Maier WD, Barnes S-J, Groves DI (2013) The Bushveld Complex, South Africa: formation of platinum–palladium, chrome- and vanadium-rich layers via hydrodynamic sorting of a mobilized cumulate slurry in a large, relatively slowly cooling, subsiding magma chamber. Mineral Deposita 48:1–56

McDonough WF, Sun S-S (1995) The composition of the Earth. Chem Geol 120:223–253

McLaren CH, De Villiers JPR (1982) The platinum-group chemistry and mineralogy of the UG-2 chromitite layer of the Bushveld Complex. Econ Geol 77:1348–1366

Merkle RKW (1992) Platinum-group minerals in the middle group of chromitite layers at Marikana, western Bushveld Complex: indications for collection mechanisms and postmagmatic modification. Can J Earth Sci 29:209–221

Mungall JE, Brenan JM (2014) Partitioning of platinum-group elements and Au between sulfide liquid and basalt and the origins of mantlecrust fractionation of the chalcophile elements. Geochim Cosmochim Acta 125:265–289

Naldrett AJ (2004) Magmatic sulfide deposits. Springer-Verlag, Heidelberg, p. 728 pp

Naldrett AJ, von Gruenewaldt G (1989) Association of Platinum-Group Elements with Chromitite in Layered Intrusions and Ophiolite Complexes. Econ Geol 84:180–187

Naldrett AJ, Kinnaird J, Wilson A, Yudovskaya M, McQuade S, Chunnett G, Stanley C (2009) Chromite composition and PGE content of Bushveld chromitites: part 1—the lower and middle groups. Appl Earth Sci 118:131–161

Naldrett AJ, Wilson A, Kinnaird J, Yudovskaya M, Chunnett G (2012). The origin of chromites and related PGE mineralization in the Bushveld Complex: new mineralogical and petrological constraints: Mineralium Deposita 47:209–232

Oberthür T, Cabri LJ, Weiser T, McMahon G, Müller P (1997) Pt, Pd and other trace elements in sulfides of the main sulfide zone, Great Dyke, Zimbabwe—a reconnaissance study. Can Mineral 35:597–609

Oberthür T, Weiser T, Gast L, Kojonen K (2003) Geochemistry and mineralogy of platinum-group elements at Hartley Platinum Mine, Zimbabwe. Miner Depos 38:327–343

Oberthür T, Junge M, Rudahevsky N, de Meyer E, Gutter P (2016) Platinum-group minerals in the LG and MG chromitites of the Bushveld Complex. South Africa – Mineral Deposita 51:71–87

Osbahr I, Klemd R, Oberthür T, Brätz H, Schouwstra R (2013) Platinum-group element distribution in base-metal sulfides of the Merensky Reef from the eastern and western Bushveld Complex, South Africa. Mineral Deposita 48:211–232

Osbahr I, Oberthür T, Klemd R, Josties A (2014) Platinum-group element distribution in base metal sulfides of the UG2, Bushveld Complex, South Africa—a reconnaissance study. Mineral Deposita 49:655–665

Osbahr I, Krause J, Bachmann K, Gutzmer J (2015) Efficient and accurate identification of platinum-group minerals by a combination of mineral liberation and electron probe microanalysis with new approach to the offline overlap correction of platinum-group element concentrations. Microsc Microanal:1–16

Pagé P, Barnes S-J, Bédard JH, Zientek ML (2012) In situ determination of Os, Ir, and Ru in chromites formed from komatiite, tholeiite and boninite magmas: implications for chromite control of Os, Ir and Ru during partial melting and crystal fractionation. Chem Geol 302-303:3–15

Penberthy CJ, Oosthuyzen EJ, Merkle RKW (2000) The recovery of platinum-group elements from the UG-2 chromitite, Bushveld Complex—a mineralogical perspective. Mineral Petrol 68:213–222

Schouwstra R, Kinloch E, Lee C (2000) A short review of the Bushveld Complex. Platin Met Rev 44:33–39

Scoates JS, Friedman RM (2008) Precise age of the platiniferous Merensky Reef, Bushveld Complex, South Africa, by the U-Pb zircon chemical abrasion ID-TIMS technique. Econ Geol 103:465–471

Scoon RN, Teigler B (1994) Platinum-group element mineralization in the critical zone of the western Bushveld Complex: I. Sulfide poor-chromitites below the UG-2. Econ Geol 89:1094–1121

Sylvania (2010) Independent metallurgical statement for the Millsell Complex as at 2nd December 2010. 8 p

Teigler B, Eales HV (1993) Correlation between chromite composition and PGE mineralization in the critical zone of the western Bushveld Complex. Mineral Deposita 28:291–302

Tredoux M, Lindsay NM, Davies G, McDonald I (1995) The fractionation of platinum-group elements in magmatic systems with the suggestion of a novel causal mechanism. S Afr J Geol 98:157–167

Vermaak C (1995) The platinum-group metals—a global perspective , 247 pMINTEK

Viljoen MJ, Schürmann LW (1998) Platinum-group metals. In: Wilson MGC, Anhaeusser CR (eds) The Mineral Resources of South Africa. Council for Geoscience. P. 532–568

Von Gruenewaldt G (1977) The mineral resources of the Bushveld Complex. Minerals Science Engineering 9:83–95

Voordouw RJ, Gutzmer J, Beukes NJ (2010) Zoning of platinum group mineral assemblages in the UG2 chromitite determined through in situ SEM-EDS-based image analysis. Mineral Deposita 45:147–159

Zientek ML, Causey JD, Parks HL, Miller RJ (2014) Platinum-group elements in southern Africa—Mineral inventory and an assessment of undiscovered mineral resources: U.S. Geological Survey Scientific Investigations Report 2010–5090–Q, 126 p.p